

Development of Robust Fuzzy Control Methods and Their Applications to a Mechanical System

G. OZMEN KOCA¹, Z. H AKPOLAT¹, M. OZDEMIR²

¹Mechatronics Engineering Department, Technology Faculty, Firat University, 23119, Elazig, Turkey

²Electrical and Electronic Engineering Department, Engineering Faculty, Firat University, 23119, Elazig, Turkey
Contact e-mail:gonca.ozmen@gmail.com

(Received: 20.12.2013; Accepted: 27.01.2014)

Abstract

In this study, a non-singleton fuzzy sliding control based strategies are investigated with simulation and also experimental studies in order to minimize angular velocity ripples of the nonlinear four-bar mechanism when it is driven by an electric motor. The mathematical model of the full system included the motor and four-bar mechanism is first obtained and open loop reply of the system is illustrated to show angular velocity ripples of the crank in the presence of the constant potential source. Secondly, an optimized PID controller by using pattern search is designed to reduce crank angular velocity ripples for the closed loop system. A new non-singleton type-1 fuzzy sliding controller is designed in order to obtain stable crank angular velocity in the steady state and performances of different types of fuzzy sliding controllers are comparatively illustrated. In addition to simulation results, experimental results of the controlled systems are also presented in order to show the effectiveness of the controllers in practice. As far as the industrial applications are concerned, simpler and more practical control algorithm is obtained with non-singleton type-1 fuzzy sliding control structure.

Key words: Four-bar linkage system, four-bar mechanism, fuzzy logic, non-singleton, sliding mode control.

Mekanik Bir Sistem için Dayanıklı Bulanık Kontrol Yöntemlerinin Geliştirilmesi ve Uygulamaları

Özet

Bu çalışmada, bir elektrik motoruyla sürülen doğrusal olmayan dört-kol mekanizmasının açılmal hız dalgalanmalarını minimuma indirmek için non-singleton bulanık kayma kipli bir kontrol uygulaması benzetim ve deneysel çalışmalarla gerçekleştirilmiştir. Öncelikle, motor ve dört-kol mekanizmasını içeren bütün sistemin matematiksel modeli çıkarılmış ve sabit kaynak gerilimi uygulandığında krank açılmal hızındaki dalgalanmaları göstermek için sistemin açık çevrim cevabı sunulmuştur. İkinci olarak, kapalı çevrim sistem için karank açılmal hızındaki dalgalanmaları azaltacak bir optimum PID kontrolör gerçekleştirilmiştir. Kalıcı durumda krank açılmal hızını sabitlemek için yeni bir non-singleton tip-1 bulanık kayma kipli kontrolör tasarlanmıştır ve farklı tip bulanık kayma kipli kontrolörlerin performansları karşılaştırılmalı olarak gösterilmiştir. Benzetim sonuçlarına ek olarak pratikte önerilen kontrolörlerin etkinliğini göstermek için kontrol edilen sistemlerin deneysel sonuçları da sunulmuştur. Endüstriyel uygulamalar göz önünde bulundurulduğunda, non-singleton tip-1 bulanık kayma kipli kontrol yapısının daha basit ve pratik olduğu sonucuna varılmıştır.

Anahtar kelimeler: Dört-kol mekanizması, bulanık mantık, non-singleton, kayma kipli control.

1. Introduction

Planar four-bar mechanisms are very important mechanisms used in machines. They can be designed to guide an extensive variety of movements and with these features such mechanisms are widely used in most industrial mechanical systems. The kinematics and

dynamics of four-bar mechanisms are most-studied topics in engineering. During analysis of these mechanisms, a confusing assumption is that the crank angular velocity is stable. The crank angular velocity has a periodic changing behavior, when a motor coupled to the mechanism. In this way, the assumption may not be the case. However, a stable crank angular

velocity is necessary [1] in order to provide timing requirement of the mechanism.

In the literature, different control methods are proposed to reduce angular velocity ripples generated by the changing inertia of the mechanism during its movement. A PID controller for the stable velocity behavior of the mechanism is developed and the simulation results are presented for the proposed controller used nonlinear techniques to determine optimal controller gain [1]. A four-bar mechanism driven by an electric motor is realized experimentally [2]. Nevertheless, the system free from real effects, friction and motor losses is designed in this study. In order to achieve better performance of the motion tracking, mass-redistribution and PD control to closed-loop mechanism are performed [3-4]. The effectiveness of the proposed methods is confirmed with simulation studies.

On the other hand, Gündoğdu and Erentürk [5] proposed a fuzzy controller in order to minimize crank angular velocity ripples of a mechanism. For quick-return mechanism, a new fuzzy neural network control method is presented [6]. An adaptive fuzzy sliding controller for a four-bar mechanism is designed by Hwang and Kuo [7] and energy based adaptive controller is modeled by Trevisani et al [8]. Moreover, a fuzzy logic control method with grey system modeling approach is applied by Erentürk [9] in order to improve angular velocity of four-bar mechanism. Ozmen Koca et al [10-11] proposed a type-2 fuzzy sliding mode control method to a four-bar mechanism to eliminate ripples of crank angular velocity. In the study, the superiority of the type-2 fuzzy sliding mode control method against type-2 fuzzy control is verified theoretically.

In this study, we added nonsingleton structure to fuzzy control systems whose inputs are modeled as fuzzy sets are also very useful to handle input uncertainties. The performances of the nonsingleton fuzzy sliding mode controllers are tested to show effectiveness of the proposed control method in order to regulate angular velocity of the mechanism with simulation and also experimental studies. Note that most of the studies about reducing velocity ripple of four-bar mechanisms present only simulation results [1,3-5,8-12]. In this study, performance of the

proposed control method is also evaluated with experimental aspects.

2. Mathematical model of the system

2.1. Mathematical model of the four-bar mechanism

Figure 1 illustrates a general structure of a four-bar mechanism. In the figure, the place of the center of mass for link i is described by r_i and θ_i and m_i represents the mass of the link. J_i and a_i are inertia moment and length of each link, respectively. In order to obtain a generalized model of the mechanism, a torsional spring and damper are added. The stiffness constant is described by k and the damping constant is described by C .

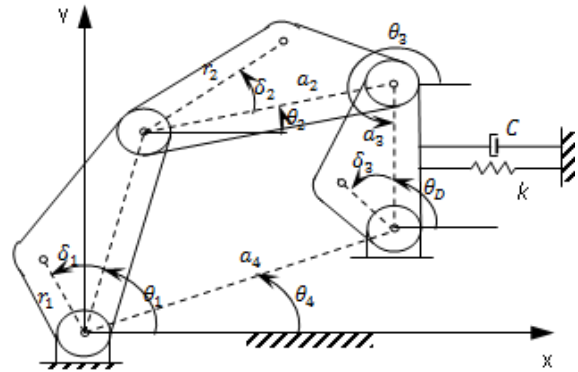


Figure 1. A general structure of a four-bar mechanism

The Lagrange's equation is given as [10]

$$\frac{d}{dt} \left(\frac{\partial K}{\partial \dot{\theta}_i} \right) - \frac{\partial K}{\partial \theta_i} + \frac{\partial P}{\partial \theta_i} + \frac{\partial D}{\partial \dot{\theta}_i} = T \quad (1)$$

where K , P and D are the kinetic, the potential and the dissipation energies, respectively. T is the applied torque. The kinetic energy of system is given as

$$K = \sum_{i=1}^3 \left[\frac{1}{2} m_i (V_{ix}^2 + V_{iy}^2) + \frac{1}{2} J_i \dot{\theta}_i^2 \right] \quad (2)$$

In the equation (2) V_{ix} is the x component and V_{iy} is the y component of the velocity and $\dot{\theta}_i$ is the angular velocity of link i . They are written as

$$\begin{aligned} V_{ix} &= u_i \dot{\theta}_1 \\ V_{iy} &= v_i \dot{\theta}_1 \\ \dot{\theta}_i &= w_i \dot{\theta}_1 \end{aligned} \quad (3)$$

In [3], the terms u_i , v_i and w_i can be achieved in detail. Also, the kinetic energy is given as [10]

$$K = \frac{1}{2} A(\theta_1) \dot{\theta}_1^2 \quad (4)$$

Where

$$A(\theta_1) = \sum_{i=1}^3 [m_i(u_i^2 + v_i^2) + J_i w_i^2] \quad (5)$$

P is given in two parts as

$$P = P_s + P_g \quad (6)$$

where (P_s) is the potential energy stored in torsional spring and (P_g) is potential energy due to the gravity and they are described as

$$P_s = \frac{1}{2} k(\theta_D - \theta_{D,0})^2 \quad (7)$$

$$P_g = \left\{ \begin{aligned} & m_1 r_1 \sin(\theta_1 + \delta_1) + m_2 (a_1 \sin \theta_1 + r_2 \sin(\theta_2 + \delta_2)) \\ & + m_3 (a_4 \sin \theta_4 + r_3 \sin(\theta_3 + \delta_3)) \end{aligned} \right\} g \quad (8)$$

where $\theta_{D,0}$ is the initial value of angular position and g is the constant of gravity. The dissipation energy from the mechanism is formed as

$$D = \frac{1}{2} C \dot{\theta}_D^2 \quad (9)$$

The equation of motion of the mechanism is obtained by substituting equations (4), (6), and (9) in equation (1) as

$$A(\theta_1) \ddot{\theta}_1 + \frac{1}{2} \frac{dA(\theta_1)}{d\theta_1} \dot{\theta}_1^2 + k \omega_3 (\theta_D - \theta_{D,0}) + C \omega_3^2 \dot{\theta}_1 = T \quad (10)$$

In [13], a full expansion of equation (10) can be found.

2.2. Mathematical model of the electric motor

Figure 2 presents a schematic of a separately-excited dc motor containing a gearbox. The gear ratio is given by

$$n = \frac{T}{T_a} = \frac{\omega_a}{\omega} \quad (11)$$

where (ω_a) is the angular velocity of shaft a , ω is the angular velocity of shaft b and T is the torque, which is the output of the motor-gear system.

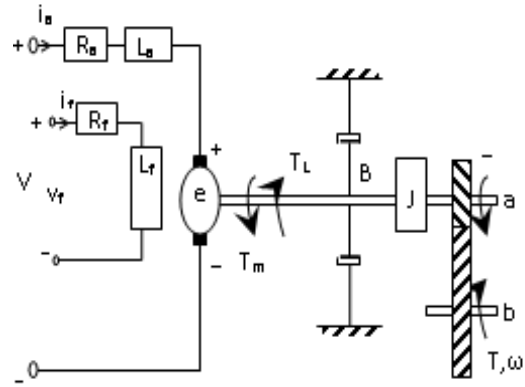


Figure 2. Schematic of a separately-excited dc motor with a gear box

In the figure, V_a is the input potential, R_a is the armature resistance, L_a is the armature inductance and i_a is the armature current. Similarly, R_f represents the field resistance, L_f is the field inductance and i_f represents the field current.

Using Kirchhoff's potential law, the potential equation is given as

$$V_a(t) = R_a i_a(t) + L_a \frac{di_a(t)}{dt} + e(t) \quad (12)$$

Where e is the generated electromotor force of the motor which is presented by

$$e(t) = K_g \omega_a(t) \quad (13)$$

Where K_g is the motor potential constant. The torque equation is written as

$$T = n(T_m - T_L - B\omega_a - J\dot{\omega}_a) \quad (14)$$

where, n is the gear ratio, J is the inertia moment, B is the coefficient of viscous friction and T_L is the load torque. T_m is the electromagnetic motor torque and it is given as

$$T_m(t) = K_m i_a(t) \quad (15)$$

Where K_m is the constant of motor torque. Since the crank of the mechanism is driven by shaft b , from equation (11) ω_a is expressed as

$$\omega_a = n\omega = n\dot{\theta}_1 \quad (16)$$

By substituting (13), (15) and (16) into (12) and (14),

$$\frac{di_a(t)}{dt} = \frac{1}{L_a} (V_a(t) - R_a i_a(t) - nK_g \dot{\theta}_1(t)) \quad (17)$$

And

$$T(t) = nK_m i_a(t) - nT_L(t) - n^2 B \dot{\theta}_1(t) - n^2 J \ddot{\theta}_1(t) \quad (18)$$

describe the mathematical model of the dc motor.

3. Control algorithm design

In this study, non-singleton fuzzy sliding mode control is proposed in order to minimize crank angular velocity ripples of the mechanism driven by an electric motor.

Type-2 fuzzy control systems can model uncertainties by using type-2 membership functions and thus these systems can minimize effects of such uncertainties [14-19]. Type-2 fuzzy control can be combined with sliding mode approach to improve the performance of the controller [10,20-26]. Since this combination also reduces the number of fuzzy rules, the controller becomes more simple and practical. Note also that non-singleton fuzzy system whose inputs are modeled as fuzzy sets are also very helpful to overcome input uncertainties. The

general form of a non-singleton fuzzy system can be presented by the same schematic block diagram of a singleton fuzzy system which can be given as Figure 3.

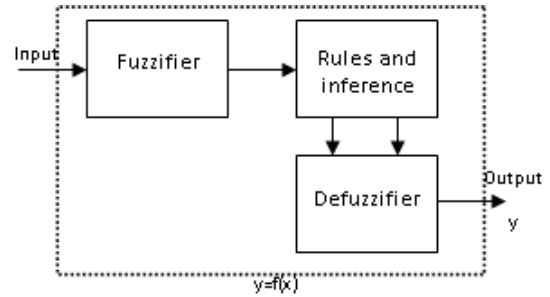


Figure 3. Schematic diagram of a singleton or a non-singleton fuzzy system [25]

In fuzzifier of a non-singleton fuzzy system, $x_i = x'_i$ is matched into a fuzzy number namely membership function $\mu_{x_i}(x'_i) = 1$ ($i = 1, \dots, p$) and when x_i moves away from x'_i which is the center value of the fuzzy sets, $\mu_{x_i}(x_i)$ decreases [14]. The shape of membership function should be symmetric about x'_i and can be chosen triangular as

$$\mu_{x_i}(x_i) = \max\left(0.1 - \left|\frac{(x_i - x'_i)}{c}\right|\right) \quad (19)$$

where c is the expanse of fuzzy sets. The general explanation of a non-singleton type-1 fuzzy system for the chosen membership function with minimum t-norm is given in Figure 4 in order to show difference between singleton structure used in the previous work [10] and non-singleton structure.

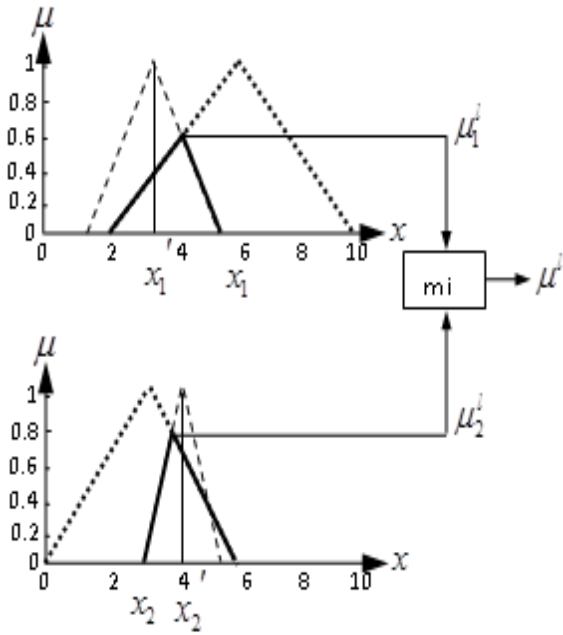


Figure 4. General explanation of input and antecedent operation for a non-singleton type-1 fuzzy system with minimum t-norm [13]

In this study, the switching function ($S = \lambda e + de$) describes the controller input and the change of reference current (Δi_{ref}) as in the previous study [10] describes the controller output. The difference is about defining the format of input, chosen as fuzzy sets, given earlier in this section.

Proposed non-singleton fuzzy sliding control structure has very successful performance which provides approximately 27% better performance about minimizing angular velocity ripples than singleton type-2 fuzzy sliding control which was proposed in the previous work [10].

The rule base of the fuzzy sliding control system is represented in Table 1.

Table 1. The rule base of the FSMC systems

S	NB	NS	ZO	PS	PB
Δi_{ref}	NB	NB	NB	NS	ZO

The rule base is obtained by considering the principal concept that a big control effect is necessary if the case is too far from the $S=0$ line and a small control effect is necessary if the case is near the $S=0$ line.

4. Simulation studies

Table 2 and 3 show the parameters of four-bar system and the DC motor used in simulations and experimental studies, respectively. The sample time of the simulation is chosen as $T_s = 2 \times 10^{-4} \text{ sec}$. The slope of the switching line (λ) is set to 20. Runge-Kutta fifth order integration method is used to perform simulations.

Table 2. Parameters of the four-bar mechanism

Link 1	Link 2	Link 3	Link 4
$a_1=0.045\text{m}$	$a_2=0.536\text{m}$	$a_3=0.272\text{m}$	$a_4=0.455\text{m}$
$r_1=0\text{m}$	$r_2=0.268\text{m}$	$r_3=0.136\text{m}$	
$m_1=1.311\text{kg}$	$m_2=0.506\text{kg}$	$m_3=0.208\text{kg}$	
$J_1=0.0019\text{kg m}^2$	$J_2=0.0167\text{kg m}^2$	$J_3=0.0058\text{kg m}^2$	

Table 3. Mechanical Properties of the DC motor

Moment of inertia	$J = 0.00051 \text{ kgm}^2$
Winding resistance	$R_a = 25.5871 \Omega$
Winding inductance	$L_a = 1.4643 \text{ H}$
Motor torque constant	$K_m = 1.0672 \text{ Nm/A}$
Motor potential constant	$K_g = 1.3758 \text{ Vs}$
Viscous friction coefficient	$B = 0.00169 \text{ Nms/rad}$

For input variables, triangular membership functions and for the output variable, singleton membership functions are chosen respectively. The range of membership functions for control systems are used as $[-20.5 \ 20.5]$ for input variable (S) and $[-1.25 \ 1.25]$ for the output variable (Δi_{ref}). The range of the membership functions are defined with steepest descent method [14].

The open loop angular velocity reply to a step input reference of 25V is presented in Figure 5. As shown in the open loop reply, the crank angular velocity has periodic changing behavior due to the effects of inertial changing of the running mechanism driven by an electric motor.

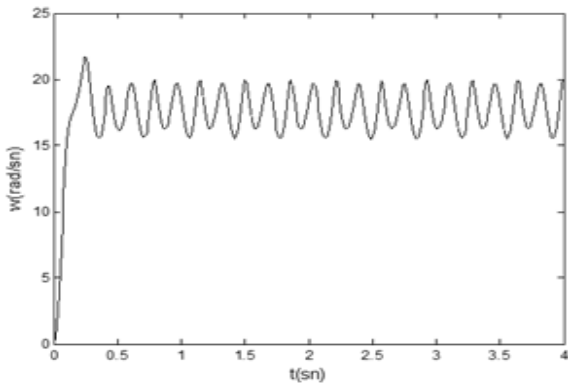
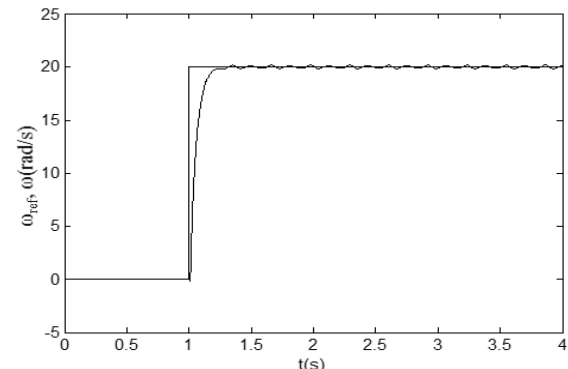
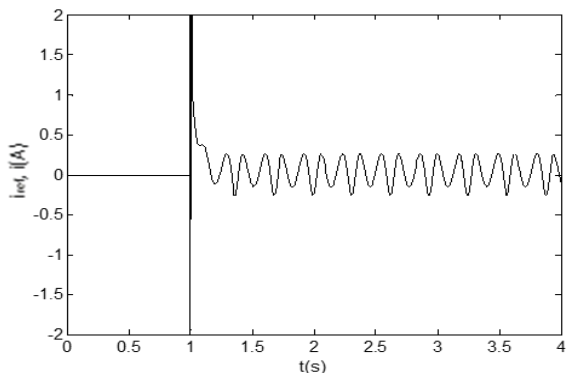


Figure 5. Open loop angular velocity reply to a step reference 25V (simulation)

An optimally tuned PID controller is tested for the complete system. The closed loop angular velocity reply to $\omega_{ref} = 20\text{rad/s}$ and the reference current is presented in Figure 6. The gains of PID controller are tuned with pattern search optimization method [1]. The controller gains are obtained as $K_p=2.382$, $K_i=0.02167$ and $K_d=0.06831$.



a)



b)

Figure 6. a) Angular velocity reply, **b)** reference current of the closed loop system for PID control (simulation)

The full system is also simulated for type-1 and type-2 fuzzy sliding control algorithms proposed in the previous work. The closed loop angular velocity errors for these control structures are shown in Figure 7 and peak to peak velocity errors are represented in Table 4.

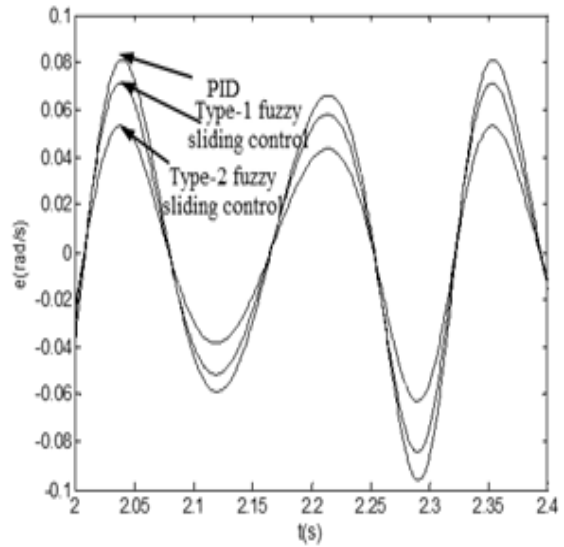


Figure 7. Closed loop velocity error for PID, type-1 and type-2 fuzzy sliding control

Table 4. Peak to peak velocity errors in the steady state

Control method	Peak to peak velocity errors (rad/s)
PID	0.1770
Type-1 fuzzy sliding	0.1556
Type-2 fuzzy sliding	0.1055

The same control parameters are used for type-1 and type-2 fuzzy control algorithms. It is clear that type-1 system provides approximately 12% better performance than PID control system and type-2 system provides approximately 30% better performance than type-1 system. Then, the fullfull system is simulated for the proposed non-singleton type-1 fuzzy sliding control method. The angular velocity reply to $\omega_{ref} = 20\text{rad/s}$ and the reference current is given in Figure 8 for the proposed control algorithm. Similarly, the non-singleton type-2 fuzzy sliding control system is also simulated and the angular velocity reply to a step reference and the reference current are presented in Figure 9.

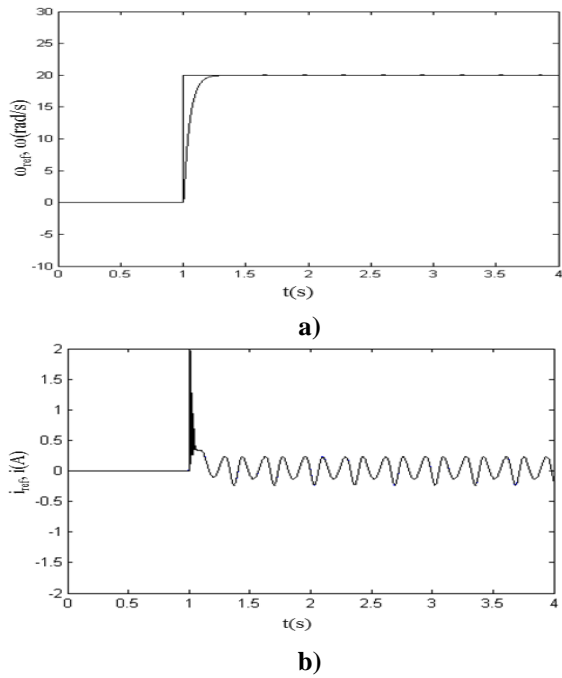


Figure 8. a) Angular velocity reply, **b)** reference current of the closed loop system for the non-singleton type-1 fuzzy sliding control

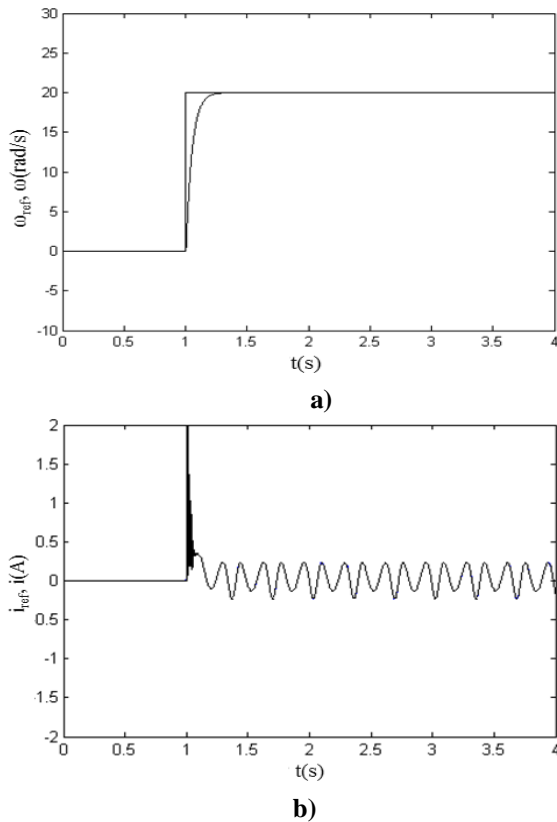


Figure 9. a) Angular velocity reply, **b)** reference current of the closed loop system for non-singleton type-2 fuzzy sliding control

The closed loop angular velocity errors for non-singleton type-1 and type-2 fuzzy sliding control systems are shown in Figure 10 and peak to peak velocity errors in the steady state for non-singleton structures are given in Table 5.

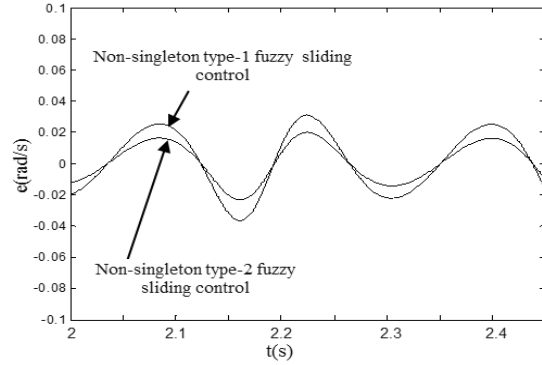


Figure 10. Closed loop velocity error for non-singleton type-1 and type-2 fuzzy sliding control

Table 5. Peak to peak velocity errors in the steady state for non-singleton structures

Control method	Peak to peak velocity errors (rad/s)
Non-singleton type-1 fuzzy sliding	0.0772
Non-singleton type-2 fuzzy sliding	0.0432

It can be understood from the Table 4 and 5 that non-singleton type-2 fuzzy sliding control system provides approximately 40% better performance than non-singleton type-1 fuzzy sliding control system and also non-singleton type-1 fuzzy sliding control system provides approximately 27% better performance about minimizing angular velocity ripples than singleton type-2 fuzzy sliding control which was proposed in the previous work. Although simulation results indicate that the best control performance is obtained by using the non-singleton type-2 fuzzy sliding control structure, the main goal of this study is to obtain more useful and simpler control algorithm which is also meaningful for experimental studies.

5. Experimental results

The experimental set block diagram is given in Figure 11. The digital signal processor

DSPACE-DS1104 is used in order to implement the control algorithm prepared at MATLAB/Simulink environment.

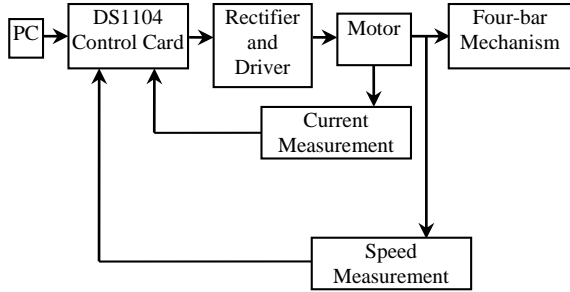


Figure 11. The block diagram of the experimental set

Experimental results are obtained by using the Control Desk Developer software which allows online access to the variables. The general view of the Control Desk Developer interface is presented in Figure 12 and the photograph of the experimental set is shown in Figure 13.

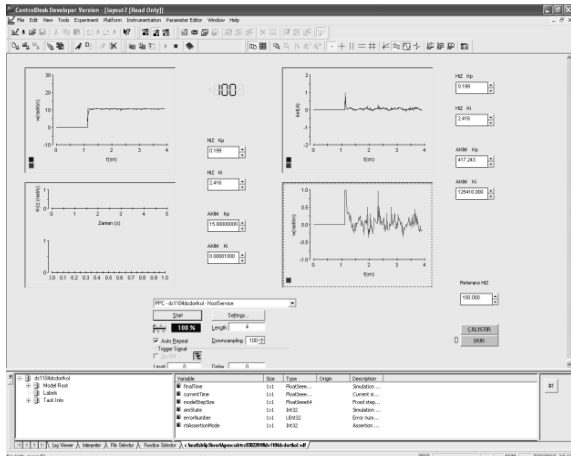


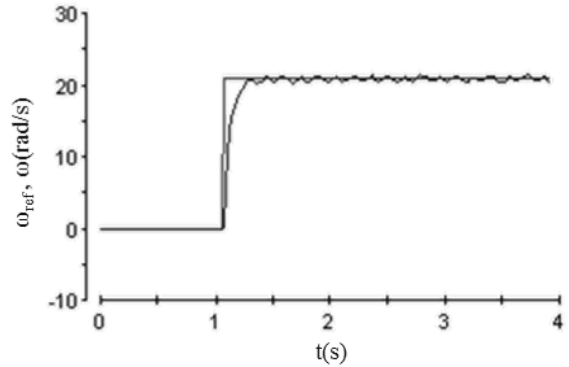
Figure 12. The general view of the Control Desk Developer interface



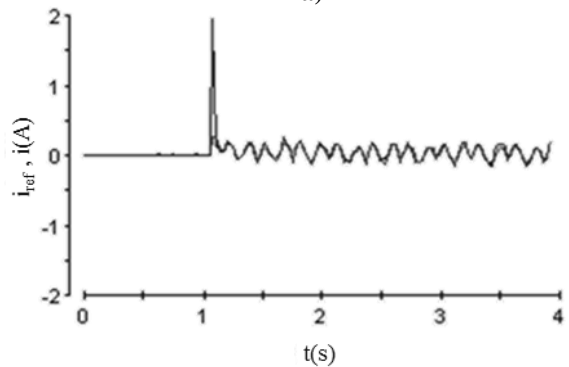
Figure 13. The photograph of the experimental set

Experimental studies are performed by using the same control parameters as used in simulation studies.

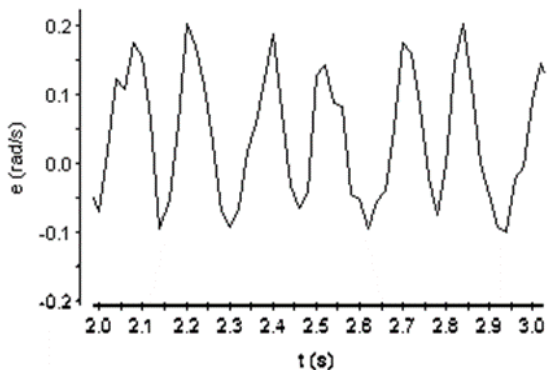
Firstly, the full system is controlled by using the non-singleton type-1 fuzzy sliding control method. The angular velocity reply to a step reference ($\omega_{ref} = 20\text{rad/s}$) is shown in Figure 14.a. The reference current and the velocity error are given in Figure 14.b and 14.c respectively.



a)



b)



c)

Figure 14. Closed loop a) angular velocity reply, b) reference current, c) velocity error of the closed loop system for non-singleton type-1 fuzzy sliding control (experimental)

The angular velocity reply to a step reference for the non-singleton type-2 fuzzy sliding control system is shown in Figure 15.a and the reference current is illustrated in Figure 15.b. The velocity error is given in Figure 15.c.

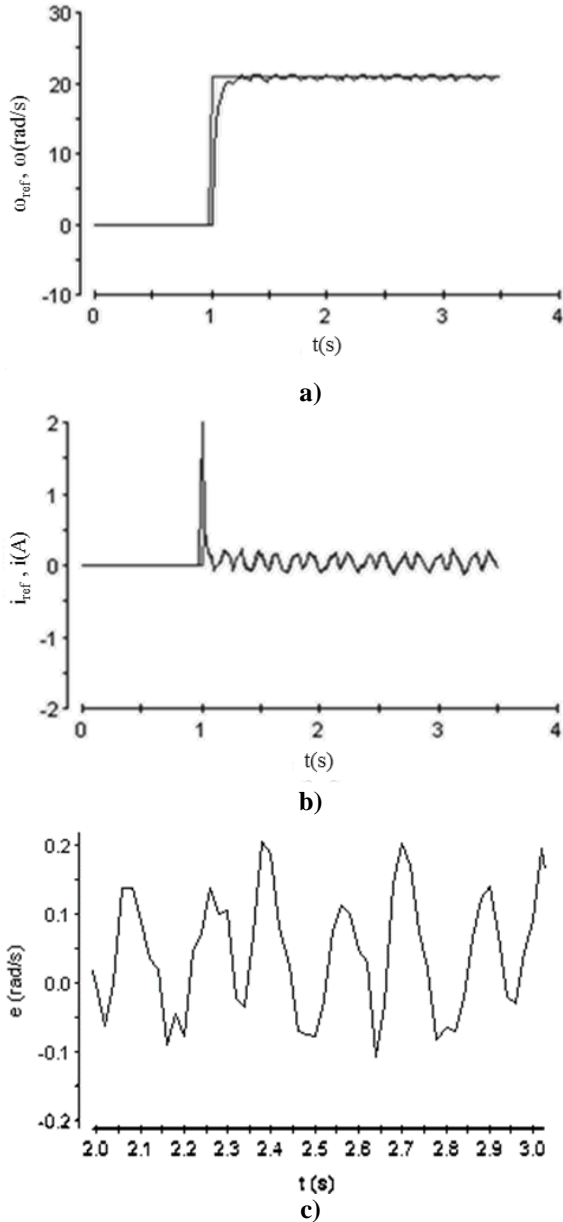


Figure 15. Closed loop a) angular velocity reply, b) reference current, c) velocity error of the closed loop system for non-singleton type-2 fuzzy sliding control (experimental)

A slightly better control performance is obtained by using the non-singleton type-2 fuzzy sliding control structure in also experimental studies. However, as seen in Figure 14 and 15,

the difference between the absolute error values of these methods is very small and it is not actually meaningful in practice.

6. Conclusions

In this paper, non-singleton type-1 and type-2 fuzzy sliding controllers are designed for the robust crank angular velocity control of the mechanism. Due to the sliding control has chattering problem when it is used in discrete time implementation, the direct application of this method to the mechanism may increase the velocity ripples on the crank angular velocity. The use of sliding mode with fuzzy logic control reduces the number of fuzzy rules and the controller becomes more simple and practical.

Non-singleton fuzzy systems whose inputs are modeled as fuzzy sets are also very useful to handle input uncertainties. The best results according to control performance are obtained using the non-singleton type-2 fuzzy sliding control structure for simulation studies. However, the control performances of both non-singleton type-1 and non-singleton type-2 fuzzy sliding controllers are superior. The error percentage and the difference between the absolute error values of these methods are very small so that it is not meaningful in practice. For this purpose, as far as the industrial applications are concerned, it is thought that the use of non-singleton type-1 fuzzy sliding control is suitable in order to have a simpler and more practical control algorithm. In other words, the new proposed combination of sliding mode and non-singleton fuzzy logic makes the control algorithm simpler and thus more practical for industrial applications. This is also supported by experimental studies in the paper.

Acknowledgements

This work is funded by Firat University Scientific Research Projects Unit. The authors would like to thank for financial support of Firat University.

7. References

1. Tao J., Sadler J. P. (1995) Constant Speed Control of a Motor Driven Mechanism System. *Mech. Mach. Theory* 30, 737–748.
2. Dulger L. C., Uyan S. (1997) Modeling, Simulation and Control of a Four-bar Mechanism with Brushless Servomotor. *Mechatronics* 7, 369–383.
3. Li Q., Tso S. K., Guo L. S., Zhang W. J. (2000) Improving Motion Tracking of Servomotor-Driven Closed-Loop Mechanisms Using mass-Redistribution. *Mech. Mach. Theory* 35, 1033–1045.
4. Zhang W. J., Chen X. B. (2001) Mechatronics Design for a Programmable Closed-Loop Mechanism. in *Proc. Inst. Mech. Eng.* 365–375.
5. Gundogdu O., Erenturk K. (2005) Fuzzy Control of a Dc Motor Driven Fourbar Mechanism. *Mechatronics* 15, 423–438.
6. Fung R. F., Lin F. J., Wai R. J., Lu P. Y. (2000) Fuzzy Neural Network Control of a Motor-Quick-Return Servomechanism. *Mechatronics*; 10, 145–167.
7. Hwang C.-L., Kuo C.-Y. (2001) A Stable Adaptive Fuzzy Sliding-Mode Control for Affine Nonlinear Systems with Application to Four-Bar Linkage Systems. *IEEE Trans. On Fuzzy Systems* 9, 238–252.
8. Trevisani A., Valcher M. E. (2005) An Energy-Based Adaptive Control Design Technique for Multibody-Mechanisms With Flexible Links. *IEEE/ASME Trans. Mech.* 10, 571–580.
9. Erentürk K. (2007) Hybrid Control of a Mechatronic System: Fuzzy Logic and Grey System Modeling Approach. *IEEE/ASME Trans. Mech.* 12, 703-710.
10. Ozmen Koca G., Akpolat Z. H., Ozdemir M. (2011) Type-2 Fuzzy Sliding Mode Control of a Four Bar Mechanism. *International Journal of Modeling and Simulation* 31, 60-68.
11. Ozmen Koca G., Akpolat Z. H., Ozdemir M. (2010) Design of a Controller Based on Type-2 Fuzzy Logic for a Four Bar Mechanism. *Firat Univ. Journal of Engineering*; 22(2), 187-195.
12. Zhang W. J., Li Q., Guo L.S. (1999) Integrated Design of Mechanical Structure and Control Algorithm for a Programmable Four-Bar Linkage. *IEEE Trans on Mechatronics* 4, 354-362.
13. Burton P. (1979) Kinematics and Dynamics of Planar Machinery. *Englewood Cliffs. NJ: Prentice-Hall.*
14. Mendel J.M. (2001) Uncertain Rule-Based Fuzzy Logic Systems: Introduction and New Directions. *Upper Saddle River. NJ: Prentice Hall PTR.*
15. Hagrass H. (2007) Type-2 FLCs: A New Generation of Fuzzy Controllers. *IEEE Computational Intelligence Magazine* 30-43.
16. Lin F.-J., Shieh P.-H., Hung Y.-C. (2008) An Intelligent Control for Linear Ultrasonic Motor Using Interval Type-2 Fuzzy Neural Network. *IET Electr. Power Appl.* 2, 32-41.
17. Karnik N. N., Mendel J. M., Liang Q. (1999) Type-2 Fuzzy Logic Systems. *IEEE Trans. On Fuzzy Systems* 7, 643-658.
18. Liang Q., Mendel J. M. (2000) Interval Type-2 Fuzzy Logic Systems: Theory and Design. *IEEE Trans. On Fuzzy Systems* 8, 535-550.
19. Mendel J. M., John R. I., Liu F. (2006) Interval Type-2 Fuzzy Logic Systems Made Simple, *Fuzzy Systems. IEEE Transactions* 14, 808-821.
20. Slotine J.J.E., Li W. (1991) Applied Nonlinear Control. *Englewood Cliffs. NJ: Prentice-Hall.*
21. Hung J.Y., Gao W.B., Hung J.C. (1993) Variable structure control: A survey. *IEEE Trans Ind Electron.* 40, 2-22.
22. Gao W.B., Hung J.C. (1993) Variable structure control of nonlinear systems: A new approach. *IEEE Trans Ind Electron.* 40, 45-55.
23. Yu X., Man Z., Wu B. (1998) Design of Fuzzy Sliding- Mode Control Systems. *Fuzzy Sets Sys.* 95, 295-306.
24. Choi B. J., Kwak S. W., Kim B. K. (1999) Design of a Single-Input Fuzzy Logic Controller and Its Properties. *Fuzzy Sets Sys.* 106, 299-308.
25. Lin P.Z., Lin C. M., Hsu C. F., Lee T. T. (2005) Type-2 Fuzzy Controller Design Using a Sliding-Mode Approach for Application to DC-DC converters. *IEE Proc.-Electr. Power Appl.* 152, 1482-1488.
26. Passino K. M. (1998) Fuzzy Control. *Addison Wesley Longman.*